Numerical analysis of vibrational generator

ZDENĚK PONČÍK, ALICE ŘIČAŘOVÁ, PAVEL FIALA
Department of Theoretical and Experimental Electrical Engineering
Faculty of Electrical Engineering and Communication, Brno University of Technology
Kolejní 4, 612 00 Brno
CZECH REPUBLIC
www.feec.vutbr.cz/UTEE

Abstract: The paper presents numerical results of the analysis of the vibrational generator. The paper deals with the design of a vibrational generator that is used as a power supply for independent electric circuits. The vibrational generator can be used in the various areas, e.g. traffic, electronics, special-purpose machines, and robotics. The proposed design employs magnetic damping of the core movement. It was numerically evaluated and it was shown that it was possible to obtain significantly larger output voltage and output power than in experimental settings used previously [1].

Key-Words: Finite element method, vibrational generator, permanent magnet, passive magnetic bearings.

1 Introduction

The development of new devices always requires a bigger emphasis on safety and reliability. One of the areas where safety demands are especially great is civil and military aircraft. Reduced reliability could lead to the heaviest losses – losses of lives.

One of the ways how to increase the safety of an aircraft is to possess a sensor net placed at critical points in the aircraft. These sensors monitor important quantities during the flight, e.g. temperature or pressure, and after the landing of an aircraft the operator just walks around the aircraft and by using wireless transmission the needed data are retrieved from all sensors. The data will be compared with those from a previous flight and all other data available.

This paper presents the results of a vibrational generator (VG) analysis. The VG is intended to provide power to sensors mentioned above. The principle of operation of a VG is based on the utilization of changes in gravity with the aid of Faraday´s law [1], [2]. The required output parameters are: output voltage between 3 – 5 V in ideal case, output power 200 – 1000 μW. The value of output power depends on the type of sensor used.

The VG body is tightly connected with the source of vibration – the fuselage, and thanks to the oscillation of the system the VG core starts moving with respect to the fuselage. The mechanical part of the VG is designed such that the VG core driven by external vibrations performs non-damped oscillations. The oscillations of the VG core are given by :

$$m \ddot{z} + l_c \dot{z} + k z = F_z \qquad (1)$$

where m is the mass of the oscillatory part of generator, l_c is the overall damping, k is the stiffness of the spring, F_z is the input force, z is the displacement in the given direction, $\dot{z}$ stands for dz/dt, and $\ddot{z}$ stands for $d^2 z/dt^2$. The design of the VG allows oscillations of the VG core within the wide spectra of external oscillation frequencies. The oscillation frequencies of the vibration source measured are given in Fig. 2.
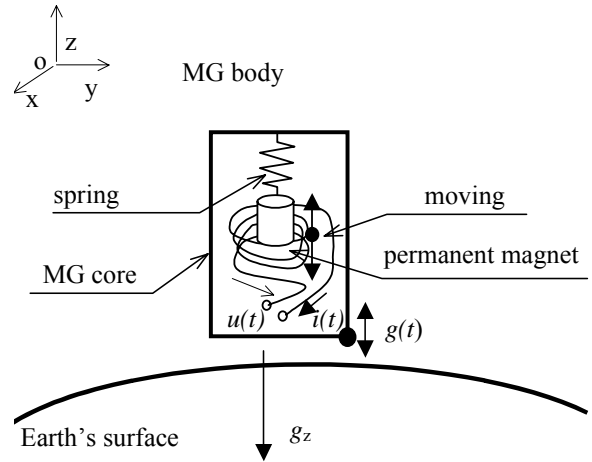

Figure 1. Basic concept of the generator

The operation of the VG is based on Faraday´s law. This fact influences the design of the magnetic circuit and the shape of the windings. There is a drawing of the principle of operation in Fig. 1. The external part of the generator is mechanically coupled to the source of vibration. This part of the VG is mechanically stiff. The VG core of mass m is connected to the mechanical stiff part of the VG by means of an elastic coupling (spring) with given damping l_c. The core is made up of the ferromagnetic material of relative permeability μ_r and permanent magnets with high density of the stored energy, e.g. FeNdB, SmCo. A voltage u(t) is induced in the winding, which is located around the movable parts of the VG. When the VG is loaded by electrical impedance, the same winding carries a current i(t).
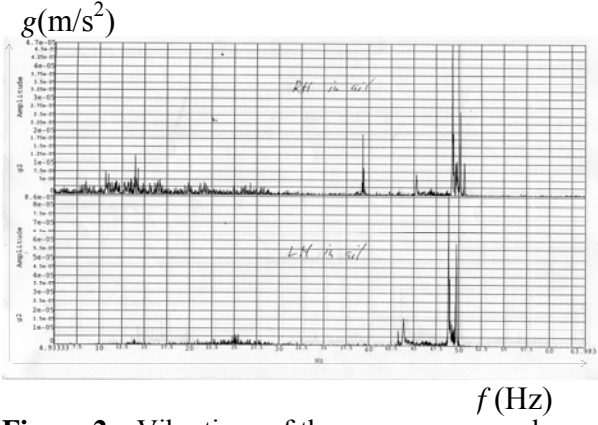
$g\,(\mathrm{m/s^2})$

$f\,(\mathrm{Hz})$

Figure 2. Vibrations of the source measured

2 Mathematical model

It is possible to carry out an analysis of the VG model using the finite element method (FEM) numerical solution. The electromagnetic part of the coupled model is described by the reduced Maxwell equations:

$$rot\ \boldsymbol{H} = \boldsymbol{J},\quad div\ \boldsymbol{B} = 0,\quad \text{in } \Omega \qquad (2),(3)$$

where $\boldsymbol{H}$ is the magnetic field intensity vector, $\boldsymbol{B}$ is the magnetic flux density vector, $\boldsymbol{J}$ is the current density vector, and Ω is the model region shown in Fig.3.

$$rot\ \boldsymbol{E} = -\frac{\partial \boldsymbol{B}}{\partial t},\quad \text{in } \Omega_w \qquad (4)$$

$$div\ \boldsymbol{J} = 0,\quad \text{in } \Omega_w \qquad (5)$$

where $\boldsymbol{E}$ is the electric field intensity vector and Ω_w is the winding region shown in Fig.4. Material relationships are represented by the equations

$$\boldsymbol{B} = \boldsymbol{H}\,\mu_0\mu_r + \mu_0\,\boldsymbol{M},\quad \text{in } \Omega_{m,fe} \qquad (6)$$

$$\boldsymbol{J}_v = \boldsymbol{E}\,\gamma,\quad \text{in } \Omega_\gamma \qquad (7)$$

where μ_0 is the permeability of vacuum, μ_r is the relative permeability, $\mu = \mu_r\mu_0$, $\boldsymbol{M}$ is the remanent intrinsic magnetisation vector of a permanent magnet, γ is the specific electric conductivity, $\Omega_{m,fe}$ is the permanent magnet region and ferromagnetic material region, and Ω_γ is the electric conductivity material region shown in Fig.4. Vector functions of an electric and a magnetic field are specified by scalar electric potential ϕ_e and vector magnetic potential $\boldsymbol{A}$

$$\boldsymbol{E} = -\mathrm{grad}\,\phi_e - \frac{\partial \boldsymbol{A}}{\partial t},\quad \text{in } \Omega_w \qquad (8)$$

$$\boldsymbol{B} = rot\ \boldsymbol{A}. \qquad (9)$$

The resulting current density vector $\boldsymbol{J}$ in equation (10) is superposed from source current density $\boldsymbol{J}_{circ}$ and eddy current density $\boldsymbol{J}_v$. The Model takes into account the core motion in that if uses current density $\boldsymbol{J}_m$.

$$\boldsymbol{J}_m = \gamma(\boldsymbol{v}\times \boldsymbol{B}),\quad \text{in } \Omega_w \qquad (10)$$

$$\boldsymbol{J} = \boldsymbol{J}_v + \boldsymbol{J}_{circ} + \boldsymbol{J}_m.\quad \text{in } \Omega_w \qquad (11)$$

After some manipulations, equations (2) to (11) yield the resultant expression for the VG mathematical model. The model's initial and boundary conditions for $i\neq j$ indexes for changes in the material on the respective border:

$$\boldsymbol{n}\times\left(\mu^{-1}\cdot rot\ \boldsymbol{A}_i\right)=0\ \text{ on border } \Gamma_1,$$

$$\boldsymbol{n}\cdot\left(\mu^{-1}\cdot rot\ \boldsymbol{A}_i\right)=0\ \text{ on border } \Gamma_2,$$

$$\boldsymbol{n}\cdot\left(\mu_i^{-1}\cdot rot\ \boldsymbol{A}_i - \mu_j^{-1}\cdot rot\ \boldsymbol{A}_j\right)=0\ \text{ on border } \Gamma_3,$$

$$\boldsymbol{n}\times\left(\mu_i^{-1}\cdot rot\ \boldsymbol{A}_i - \mu_j^{-1}\cdot rot\ \boldsymbol{A}_j\right)=0\ \text{ on border } \Gamma_4,$$

$$\boldsymbol{n}\times\left(-\gamma_i\cdot grad\varphi_i + \gamma_j\cdot grad\varphi_j\right)=0\ \text{ on border } \Gamma_5,$$

$$\boldsymbol{n}\times\left(grad\varphi_i\right)=0\ \text{ on border } \Gamma_6,$$

$$\boldsymbol{n}\times\left(-\gamma_i\cdot\frac{\partial \boldsymbol{A}_i}{\partial t} + \gamma_j\cdot\frac{\partial \boldsymbol{A}_j}{\partial t}\right)=0\ \text{ on border } \Gamma_7,$$

$$\boldsymbol{n}\times\left(\frac{\partial \boldsymbol{A}_i}{\partial t}\right)=0\ \text{ on border } \Gamma_8, \qquad (12)$$

$$\Gamma\subset\bigcup_{k=1}^{8}\Gamma_k\ ,\ \Gamma \text{ is border of region } \Omega.$$

$$\varphi(t_0,x,y,z)=\varphi_0(x,y,z),\quad x,y,z\subset\Omega,$$

$$\frac{\partial\varphi}{\partial t}(t_0,x,y,z)=\frac{\partial\varphi_0}{\partial t}(x,y,z),\quad x,y,z\subset\Omega,$$

$$\boldsymbol{A}(t_0,x,y,z)=\boldsymbol{A}_0(x,y,z),\quad x,y,z\subset\Omega,$$

$$\frac{\partial \boldsymbol{A}}{\partial t}(t_0,x,y,z)=\frac{\partial \boldsymbol{A}_0}{\partial t}(x,y,z),\quad x,y,z\subset\Omega. \qquad (13)$$

After applying of the Gallerkin method, manipulating relations (2)-(13), taking into account the material properties, taking into account of initial and boundary conditions, we obtain the resultant mathematical model of the coupled electromagnetic and mechanic problem (15).

$$\left[l_{AJ}\right]\{\dot{a}\} + \left[k_{A\varphi J}\right]\{\varphi\} = \left[z_{\varphi\varphi}\right]\{\rho\},\quad i,j=1,..,N_u, \qquad (14)$$

$$\begin{bmatrix}L_A+L_{A\varphi} & 0 & 0\\ 0 & 0 & 0\\ 0 & 0 & -\Theta L_S\end{bmatrix}\begin{Bmatrix}\dot{a}\\ \dot{\phi}\\ \dot{S}\end{Bmatrix} + \begin{bmatrix}K_{A1}+K_{A2}-(1-\Theta)K_{A3} & 0 & 0\\ 0 & K_\varphi+K_{\varphi\varphi} & 0\\ 0 & 0 & 0\end{bmatrix}\begin{Bmatrix}a\\ \phi\\ S\end{Bmatrix}$$

$$= \begin{bmatrix}z_J & z_{\varphi\varphi} & 0\\ 0 & 0 & 0\\ 0 & 0 & 0\end{bmatrix}\begin{Bmatrix}j_s\\ \rho\\ 0\end{Bmatrix} + \begin{bmatrix}z_M & 0 & 0\\ 0 & 0 & 0\\ 0 & 0 & 0\end{bmatrix}\begin{Bmatrix}m\\ 0\\ 0\end{Bmatrix}$$

$$\qquad (15)$$

where L_A, $L_{A\varphi}$, L_S, K_A, K_{A2}, K_{A3}, K_φ, and $K_{\varphi\varphi}$ are the local matrixes of the coefficients, z_j, $z_{\varphi\varphi}$, and z_M are the matrixes of electromagnetic field sources, j_c is the column vector of the current densities, m is the mass column vector, a is the column vector of the unknown vector magnetic potentials of the discretized model, ϕ is the column vector of the unknown scalar electric potentials of the discretized model, S is the column vector of the unknown movement vectors of the discretized model, and $\dot{a}, \dot{\phi}, \dot{S}$ are the time derivatives of the column vectors of potentials and movements.

3 FEM model in ANSYS program

The geometrical model was created with standard tools in the ANSYS program [5] and with the aid of automated mesh generator. The element applied is SOLID97. The ferromagnetic material is non-linear with the B-H curve of steel as given by the ČSN 15670 standard. The properties of the SmCo permanent magnet were taken over from the data sheet of the magnet manufacturer. The model in ANSYS is described by the characteristic data:

DISPLAY FEM MODEL SIZE INFORMATION
***** FEM MODEL SIZE *****

Maximum Node Number	=	90489
Number of Defined Nodes	=	90489
Maximum DOF per Node	=	3
Maximum Element Number	=	91780

In Figure 4 one can see the geometrical characteristics from the VG model. It consists of passive magnetic bearings and additional magnetic circuits. These mainly influence the function of the vibrational VG [3].

4 Results of static analysis

The modules of vector functions of magnetic field density B and intensity H are shown in Fig.5. For a correct model design it is necessary to evaluate the distribution of forces. These were gained from virtual works given in Fig.6. The model is fully 3D. No symmetries used in the model. This is due to the convergence evaluation and error estimation [6], [7].

5 Conclusion

The present study is a part of an introductory study of the vibrational generator design. It is intended as a preparation for a proposed 6th General European Project.
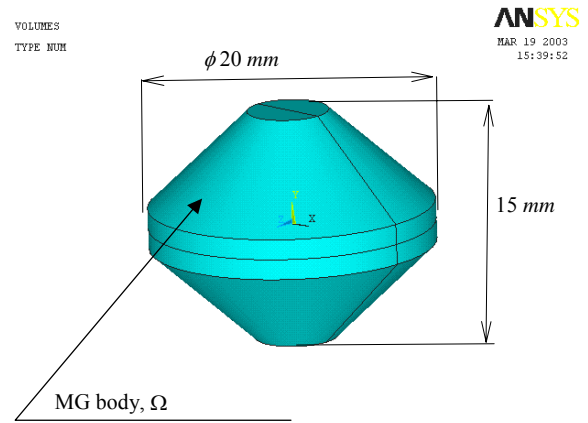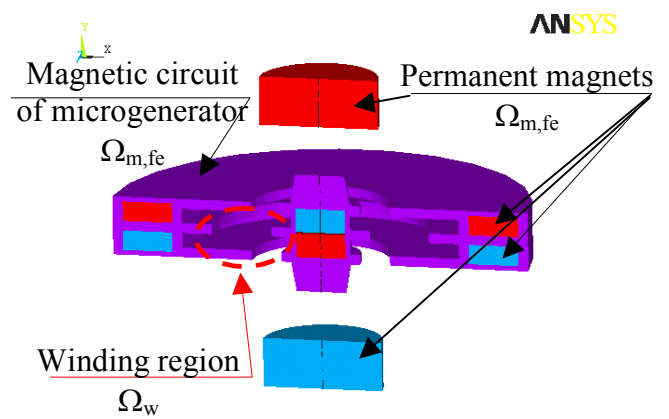

Figure 3. Geometrical model of VG

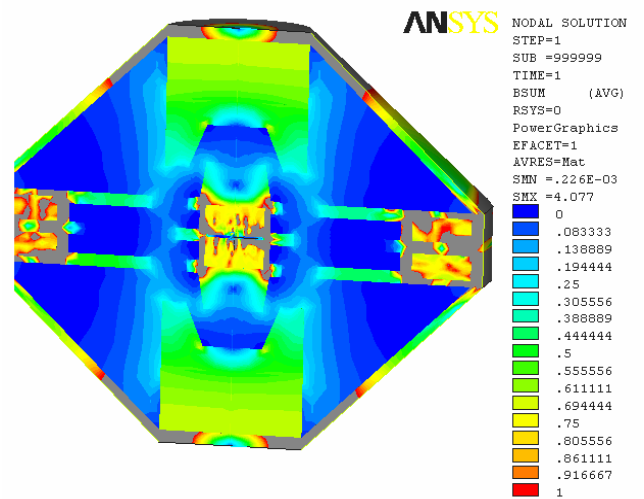**Figure 4.** Geometrical model of generator

Figure 5. Evaluation of modules of magnetic field density B
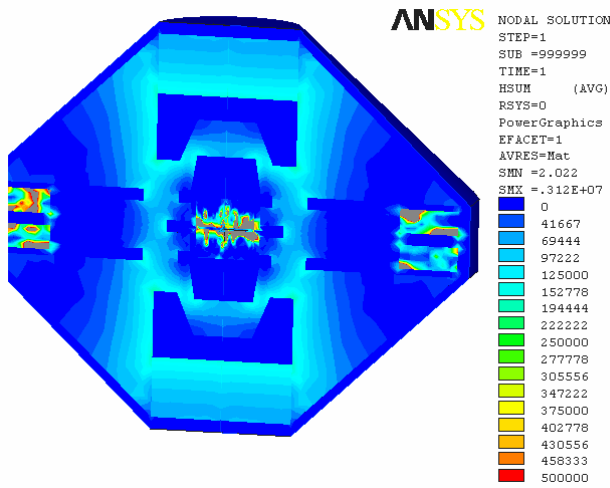
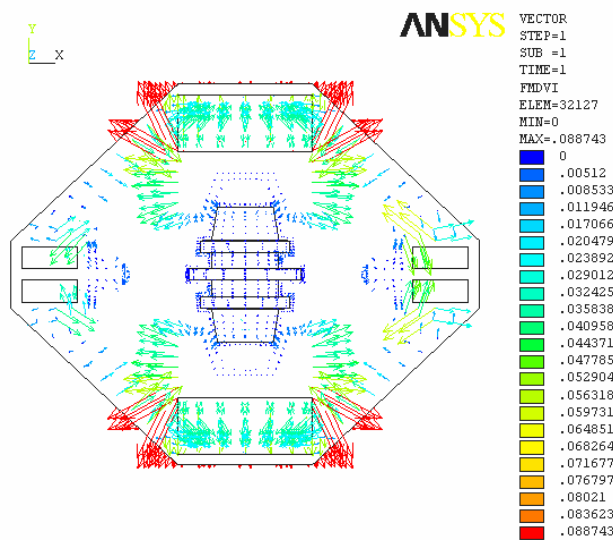**Figure 5.** Evaluation of modules of magnetic field intensity *H*.

Figure 6. Evaluation of vector of relative forces *f* existing in VG body
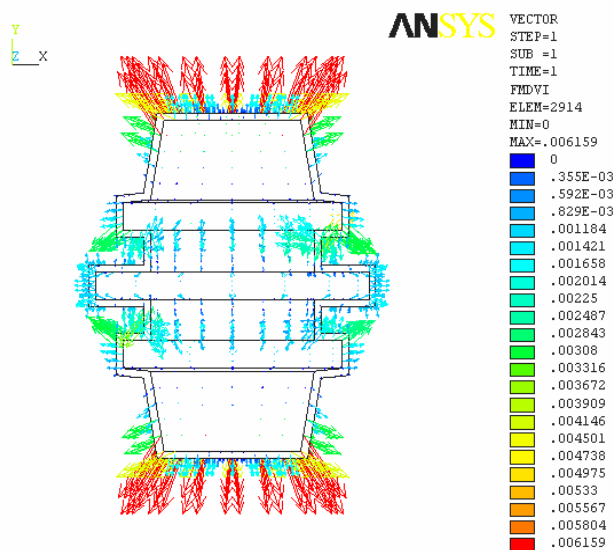

Figure 6. Evaluation of vector of relative forces *f* existing in VG body

The analysis has shown that it is possible to suitably change the shape of the generator magnetic circuit. The paper presents results of the distribution of magnetic and electric field intensities and densities. In order to get the required voltage *u(t)* it is possible to suitably modify the shape of the winding (details are discussed in [4]). The basic estimates of the effect of the forces on the magnetically damped VG core have been obtained. The VG model is ready for transient simulations. The first step towards the time domain simulations is the computation of the lumped parameters of the model. The time domain simulations were performed using the lumped equivalent circuit in the MATLAB program. This approach is not very accurate in comparison with FEM capabilities. However, this approach is substantially faster. The results of the analysis serve as a foundation for the design of the generator.

References:

[1] Wen,J.Li-Z. Wen, -P.K.Wong A micromachined vibration induced power generator for low power sensors of robotic systems. *World Automation Congress*, Maui, Hawai, June 11.-16. Juli 2000.

[2] Stratton,J.A, *Teorie elektromagnetického pole*. SNTL Praha 1961.

[3] Řičařová,A., *Mikrogenerátor o výkonu 1mW*. Diploma work, FEKT VUT v Brně, 15.6.2003.

[4] Fiala,P., *Conception of vibrational microgenerator*, Research report, 30.1.2003, UTEE FEKT v Brně, str.102.

[5] ANSYS, *User´s manual for revision 5.1-8.0, Volume I-IV*, Swanson Analysis System, Inc., Houston, Usa, 1994-2003.

[6] Fiala,P.: *Modelling of short circuit transformes tests*, Doctor work, UTEE FEI VUT v Brně, 30.12.1998, UTEE FEKT v Brně.

[7] Fiala, P.: *Solution of electric field at a bushing support from distribution frame*, Research report no.1/96, Laboratoř modelování a optimalizace polí v elektromechanických systémech FEI VUT BRNO a ABB EJF, a.s. BRNO, 24.7.19